Supporting Information

Stabilizing Ni catalysts in biogas reforming via In-Situ carbon deposit removal by CeO_2 oxygen vacancies

Yonggang Gang[a], Zijiang Zhao[a], Yanhui Long[a], Xiaodong Li[a], Hao Zhang*[,a]

[a]State Key Laboratory of Clean Energy Utilization, Zhejiang University, Hangzhou 310027, China

* Corresponding author:

zhang_hao@zju.edu.cn (H. Zhang)

Table of Contents

Preparation of Catalysts

Ni_3Fe/CeO_2

Firstly, CeO_2 was prepared by weighing 4.0 g of $Ce(NO_3)_3 \cdot 6H_2O$, adding 100 ml of deionized water to make a solution, and then stirring for 30 min at room temperature, followed by dropping ammonia to make the PH value reach 9.5-10, stirring at room temperature overnight, and then finally filtering and washing the precipitate, drying it for 12 h in the oven at 80 °C, and then finally calcining it for 5 h at a temperature of 950 °C (10 °C/min), to obtain CeO_2. Ni_3Fe/CeO_2 was prepared using the impregnation method, the total nickel-iron metal loading was set at 10 wt%, and then a certain amount of $Ni(NO_3)_2 \cdot 6H_2O$ and $Fe(NO_3)_3 \cdot 9H_2O$ were weighed according to the proportion as the metal precursor, and a solution was made by adding deionized water and ethanol (1:1) and stirred at room temperature for 30 min, 1 g of CeO_2 was added, stirred and dried, and then the final precipitate obtained was calcined in a muffle furnace at a temperature of 400 °C (5 °C/min) calcined for 4h.

Ni_3Fe/CeO_2-NS

4 g of $Ce(NO_3)_3 \cdot 6H_2O$ and 4 ml of deionized water were combined to form solution A. Subsequently, 4 ml of glacial acetic acid and 104 ml of ethylene glycol were mixed to create solution B. Both solutions were stirred separately before A was added to B, with stirring continuing for 30 minutes. The mixture was then transferred to a 100 ml autoclave, where it underwent hydrothermal processing at 100°C for 24 hours. The resultant solid was isolated, dried, and calcined following the same procedure to obtain CeO_2-nanostructure (remarked as CeO_2-NS). Ni_3Fe/CeO_2-NS was synthesized using the impregnation method previously described.

Ni_3Fe/CeO_2-RS

Ni_3Fe/CeO_2-rod structure (regarded as Ni_3Fe/CeO_2-RS) was synthesized using the hydrothermal precipitation method. A solution was prepared by dissolving 16.8 g of NaOH in 70 ml of deionized water (solution a). Concurrently, the metal precursor

(0.004 mol) was dissolved in 10 ml of deionized water to form another solution (solution b). Both solutions were stirred separately before solution a was added to solution b, and the mixture was stirred for an additional 30 minutes. This mixture was then transferred to a 100 ml autoclave for hydrothermal treatment at 120 °C for 24 hours. The resultant solid was isolated and dried following the same procedure used for CeO_2 preparation and then calcined at 400 °C for 2 hours.

Characterizations

The contents of the metals Ni and Fe were determined by inductively coupled plasma optical emission spectroscopy (ICP-OES, Agilent S730, USA).

Nitrogen adsorption/desorption measurements were used to determine the physical properties of the catalysts produced. Parameters studied included total surface area, pore size distribution and pore volume. The Brunauer-Emmett-Teller (BET) method was used to calculate the surface area and the Barrett, Joyner and Halenda (BJH) method was used to study the mesoporosity. Measurements were made using a fully automated BET (Quantachrome Autosorb IQ3, USA) dedicated surface and porosity analyser.

Powder X-ray diffraction (XRD) studies were carried out on a Rigaku SmartLab SE diffractometer using copper target radiation. X-ray diffractograms were recorded between $2\theta = 10 - 80°$ at a rate of 2 °/min.

Transmission electron microscopy (TEM) was used to analyse the morphology of fresh and post-reaction catalyst samples for analysis using FEI Talos F200x, USA. In addition, mapping tests were performed to check the distribution of elements in the samples.

X-ray photoelectron spectroscopy (XPS) was performed using Al Ka radiation (Thermo Scientific K-Alpha, USA). 284.8 eV C 1s signals were used to calibrate binding energies for all spectra. For each depleted catalysis, a high-resolution area scan and a low-resolution survey were performed to determine the associated binding energy.

TGA tests were carried out using Netzsch TG 209 F3 Tarsus, Germany, to investigate the type and amount of carbon build-up on the spent catalyst. The rate of temperature increase was 10 °C min^{-1}, from 50 °C to 800 °C.

Catalytic Evaluations

The catalyst performance experiment was carried out in a quartz tube with a length of 600 mm and an inner diameter of 8 mm, and the pressure was normal. 0.1 g of catalyst (40-60 mesh) was diluted with 0.9 g of quartz sand. Before the reaction, the catalyst was reduced at 700 ℃ with a mixed gas of hydrogen and argon (H_2 : 20 %) for 1 hour. Nitrogen was introduced, the temperature was raised to 800 ℃, and the mixture of CH_4 and CO_2 (CH_4: CO_2: N_2 = 3 : 2 : 5, total flow rate was 100 ml/min) was introduced. The analysis was carried out by an online gas chromatograph (FULI GC9790) fitted with FID and TCD detectors. Cycling performance experiments were conducted in the same way as described above, with the reaction gas switched to CO_2 after 3h of feed, and switched to reaction gas again after 1 hour of CO_2 reaction.

CH_4 conversion, CO_2 conversion and reaction rate are calculated according to the following formula:

The conversion of CH_4 (X_{CH4}) is defined as

$$X_{CH_4}(\%) = \frac{moles\ of\ CH_4\ converted}{moles\ of\ initial\ of\ CH_4} \times 100 \qquad (S1)$$

The conversion of CO_2 (X_{CO2}) is defined as

$$X_{CO_2}(\%) = \frac{moles\ of\ CO_2\ converted}{moles\ of\ initial\ of\ CO_2} \times 100 \qquad (S2)$$

The H_2/CO is defined

$$\frac{H_2}{CO} ratio = \frac{moles\ of\ H_2\ producted}{moles\ of\ CO\ \ producted} \qquad (S3)$$

The C balance is defined as

$$C_{balance} = \frac{[moles\ of\ CH_4]_{out} + [moles\ of\ CO]_{out} + [moles\ of\ CO_2]_{out}}{[moles\ of\ CH_4]_{in} + [moles\ of\ CO_2]_{in}} \times 100\% (S4)$$

Where [moles of X] $_{in}$ and [moles of X] $_{out}$ represent the moles of X before and after reactions, respectively.

The carbon deposition rate, defined as Eq S5, represents the amount of carbon deposited on the catalyst surface per unit time.

$$\text{the carbon deposition rate} = \frac{mass\ of\ carbon\ (mg)}{mass\ of\ catalyst\ (g) * reaction\ time\ (h)} \quad (S5)$$

Where the mass of carbon is the amount of carbon deposited on the catalyst's surface after the reaction, and the mass of the catalyst is the mass used in the TGA analysis.

Figures S1-S12 and Table S1-S2

Table S1 Texture properties and metal loading weight of the fresh samples

Sample	Ni loading (wt%) [a]	Fe loading (wt%) [a]	Surface Area (m^2g^{-1}) [b]	Pore Diameter (nm) [b]	Pore Volume (cm^3/g) [b]
Ni_3Fe/CeO_2	6.32	2.06	2.02	11.58	0.005
Ni_3Fe/CeO_2-NS	8.54	2.83	11.17	12.21	0.055
Ni_3Fe/CeO_2-RS	8.42	2.80	13.54	42.11	0.227

a measured by ICP-OES
b calculated by BET formular

Table S2 Oxygen vacancy concentration and biogas reforming CH_4 and CO_2 conversion

Sample	Ce^{3+} / (Ce^{3+} + Ce^{4+}) [a]	initial CH_4 conversion (%) [b]	final CH_4 conversion (%) [b]	initial CO_2 conversion (%) [b]	initial CO_2 conversion (%) [b]
Ni_3Fe/CeO_2-600	0.21	71.1	40.3	94.5	58.7
Ni_3Fe/CeO_2-500	0.23	76.9	52.2	88.5	76.1
Ni_3Fe/CeO_2-NS	0.28	84.7	65.8	96.7	95.9
Ni_3Fe/CeO_2-RS	0.33	80.4	67.7	97.2	94.4

a measured by XPS

b obtained by experiment

Ni_3Fe/CeO_2-x refers to a reduction temperature of x degrees before reaction

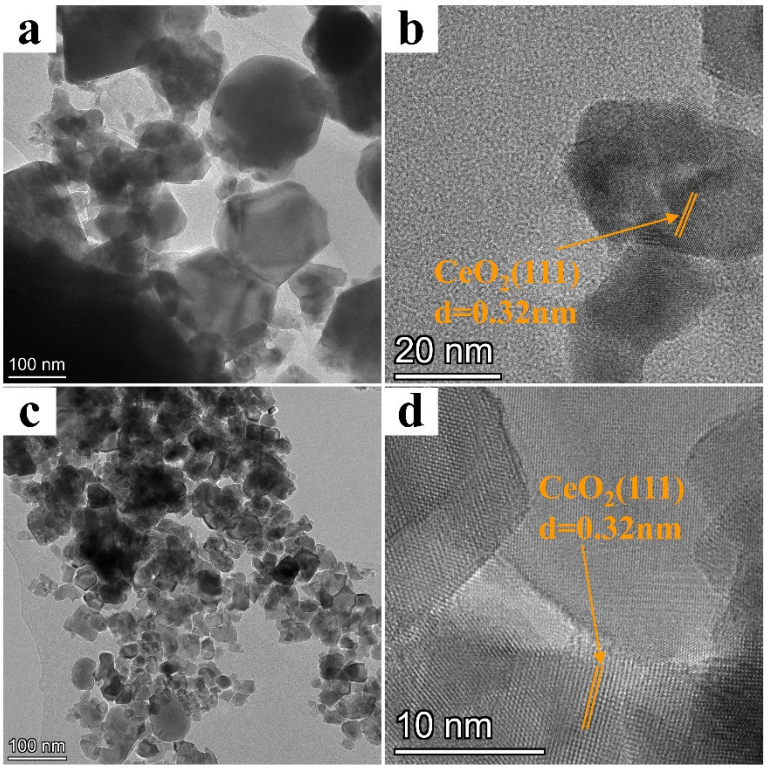

Fig. S1 TEM images of the catalyst before the reaction and the corresponding exposed crystal face information. a-b: Ni_3Fe/ CeO_2, c-d: Ni_3Fe/CeO_2-NS.

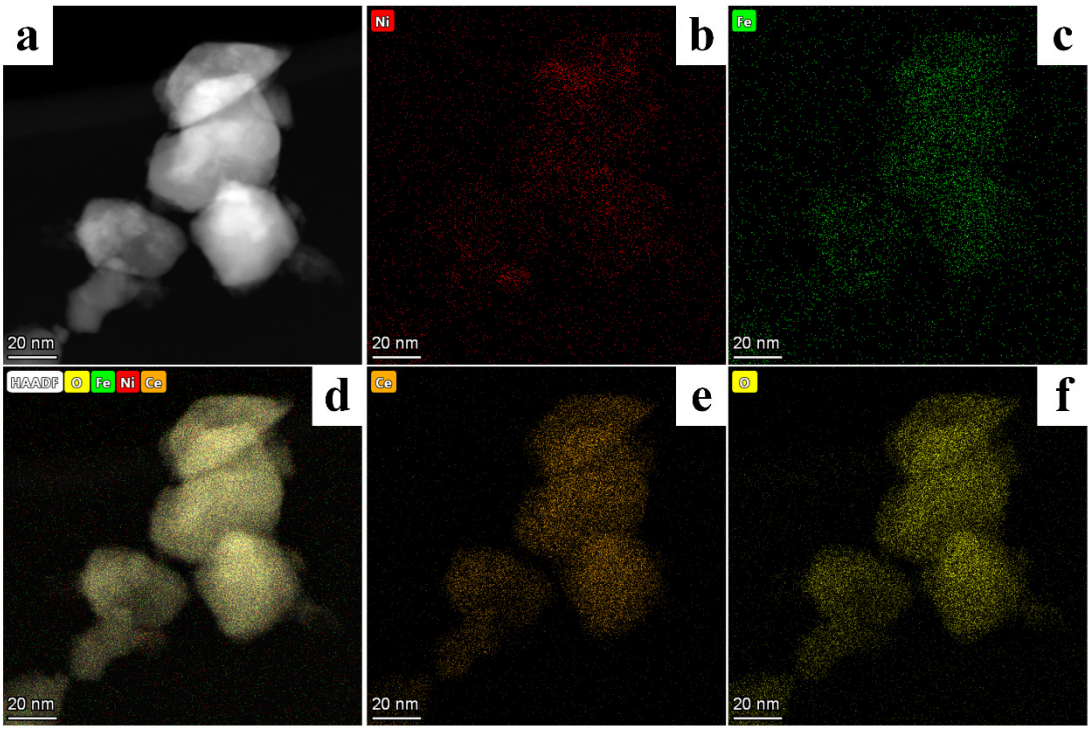

Fig. S2 HAADF-STEM images and mapping images of the fresh Ni_3Fe/CeO_2 catalyst.

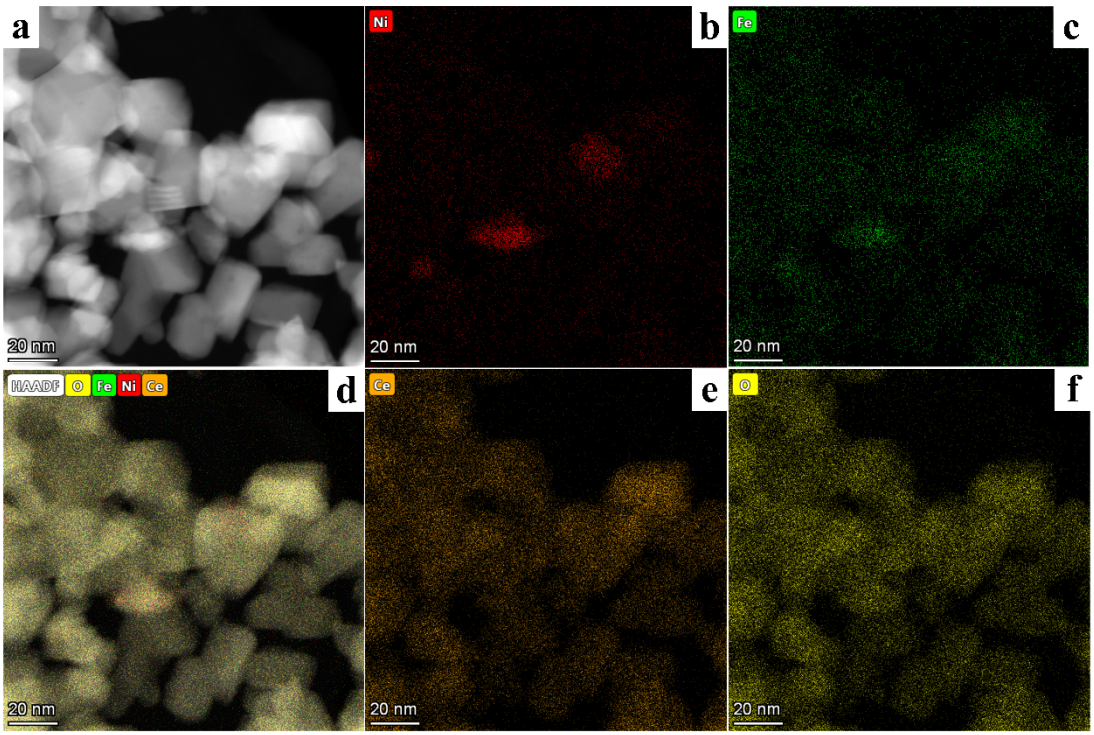

Fig. S3 HAADF-STEM images and mapping images of the fresh Ni_3Fe/CeO_2-NS catalyst.

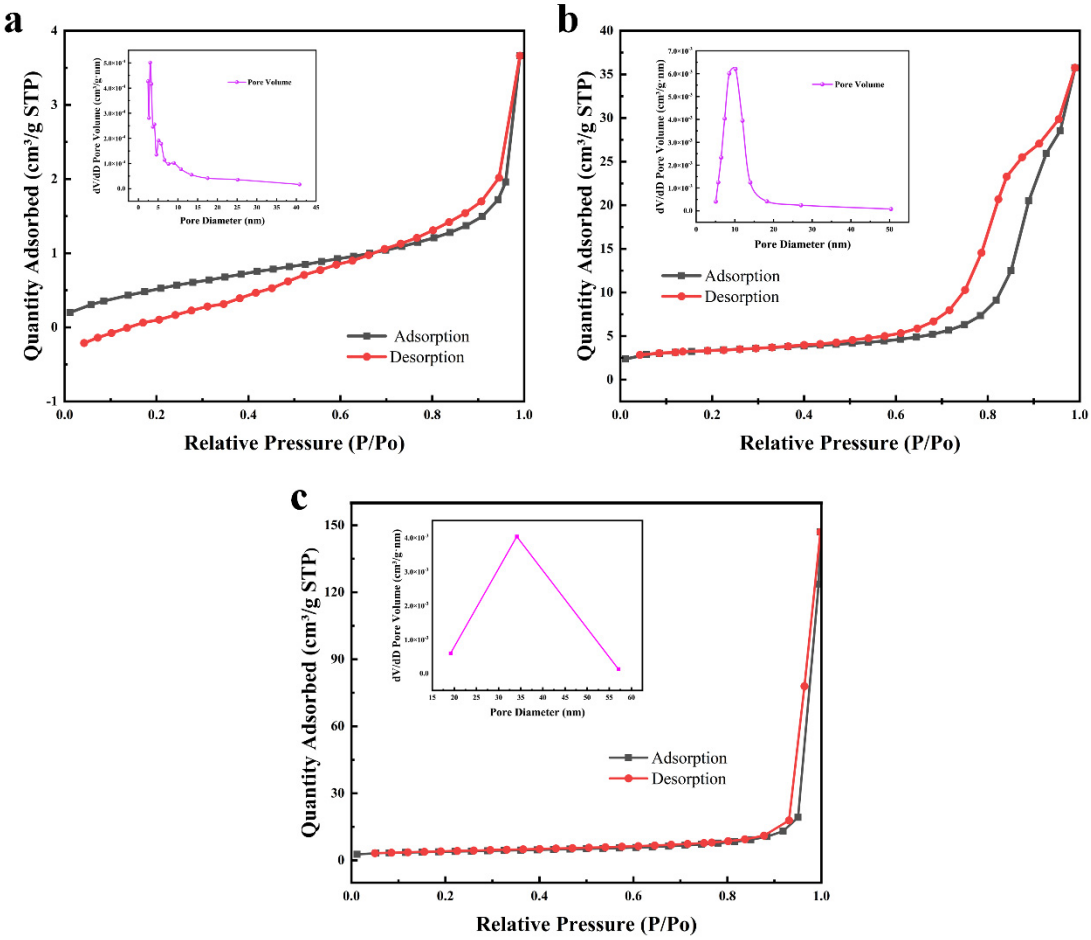

Fig. S4 N_2 sorption isotherms and pore diameter distribution of Ni_3Fe/CeO_2 (a), Ni_3Fe/CeO_2-NS (b) and Ni_3Fe/CeO_2-RS (c), respectively.

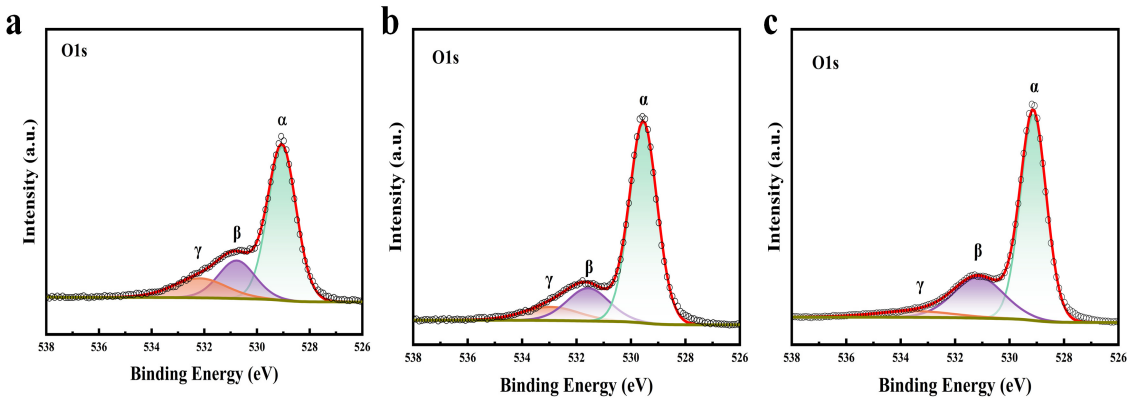

Fig. S5 O 1s XPS spectrums of Ni_3Fe/CeO_2 (a), Ni_3Fe/CeO_2-NS (b) and Ni_3Fe/CeO_2-RS (c), respectively.

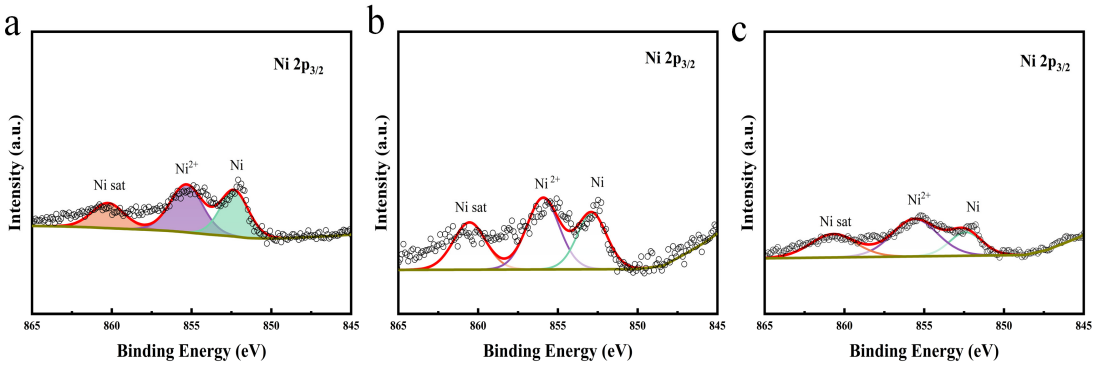

Fig. S6 Ni 2p XPS spectrums of Ni_3Fe/CeO_2 (a), Ni_3Fe/CeO_2-NS (b) and Ni_3Fe/CeO_2-RS (c), respectively.

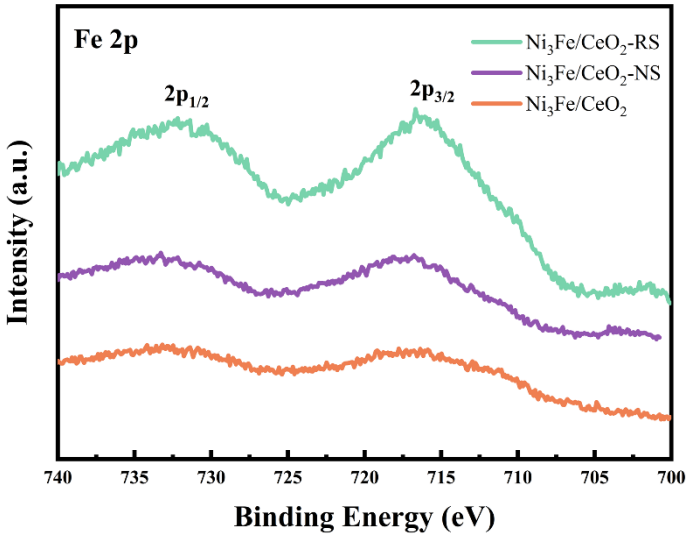

Fig. S7 Fe 2p XPS spectrums of the catalysts.

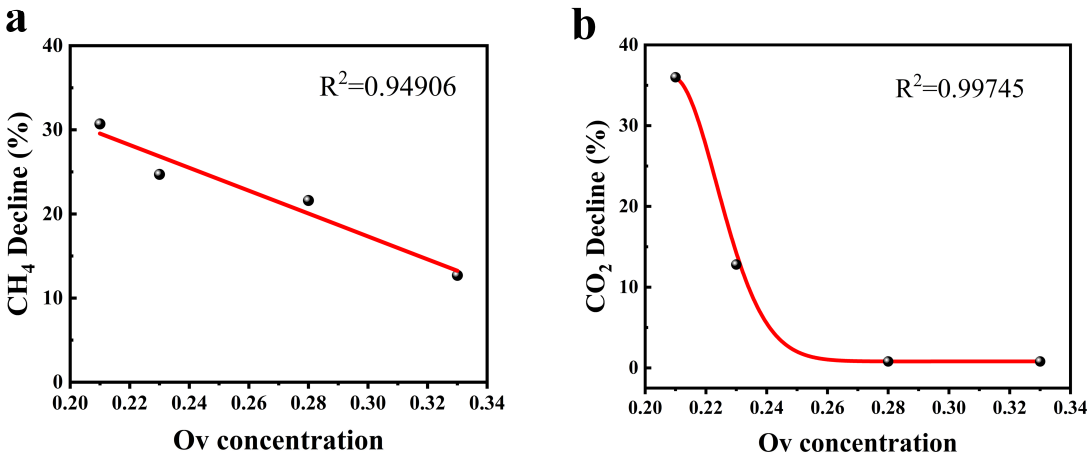

Fig. S8 Relationship between Ov concentration and decline of CH_4 and CO_2 conversion.

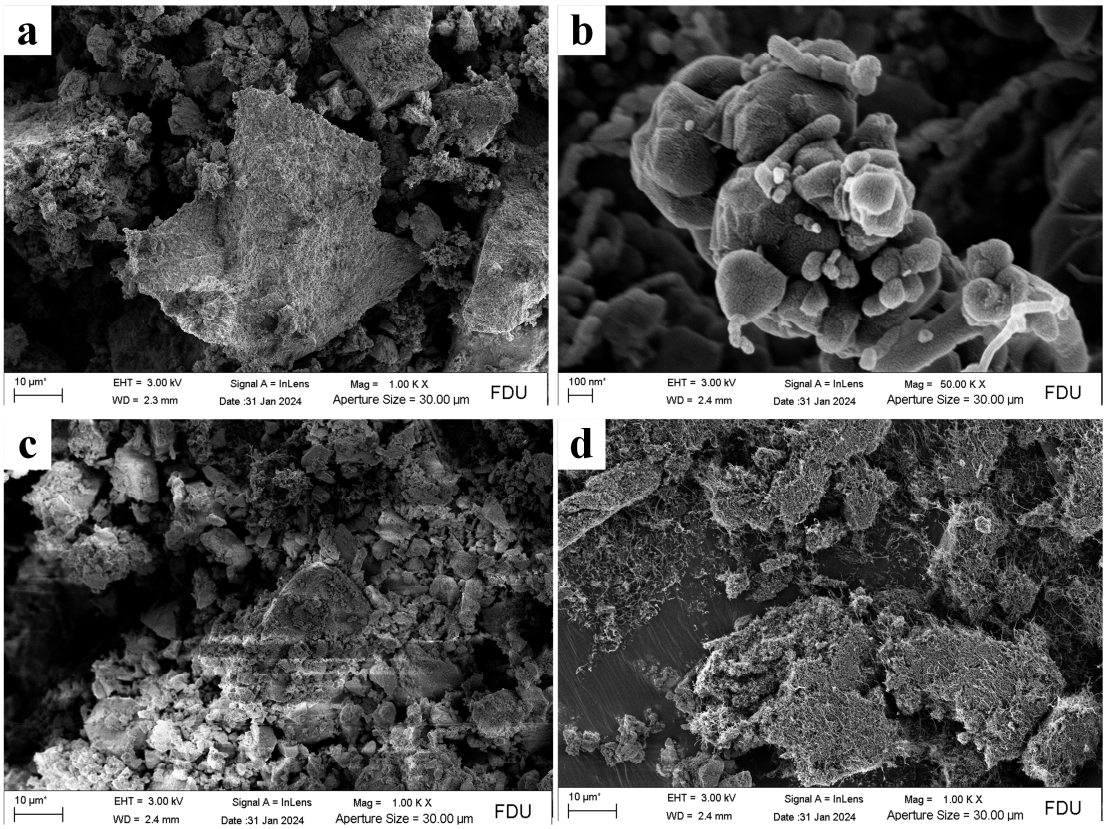

Fig. S9 SEM images of fresh and spent catalysts, Ni_3Fe/CeO_2 (a-b), Ni_3Fe/CeO_2-NS (c-d).

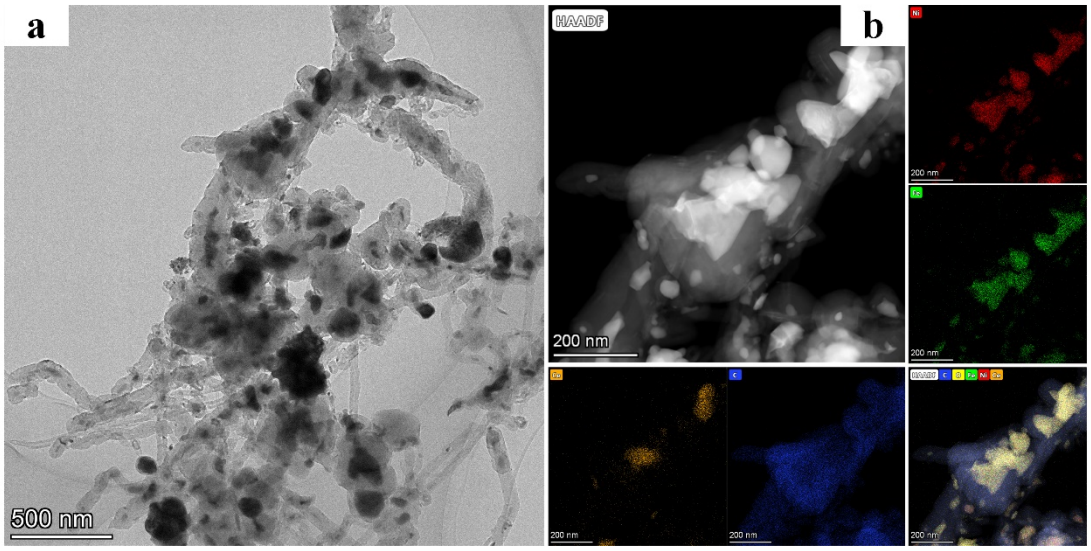

Fig. S10 TEM (a) HAADF-STEM images and mapping (b) images of the spent Ni_3Fe/CeO_2 catalyst.

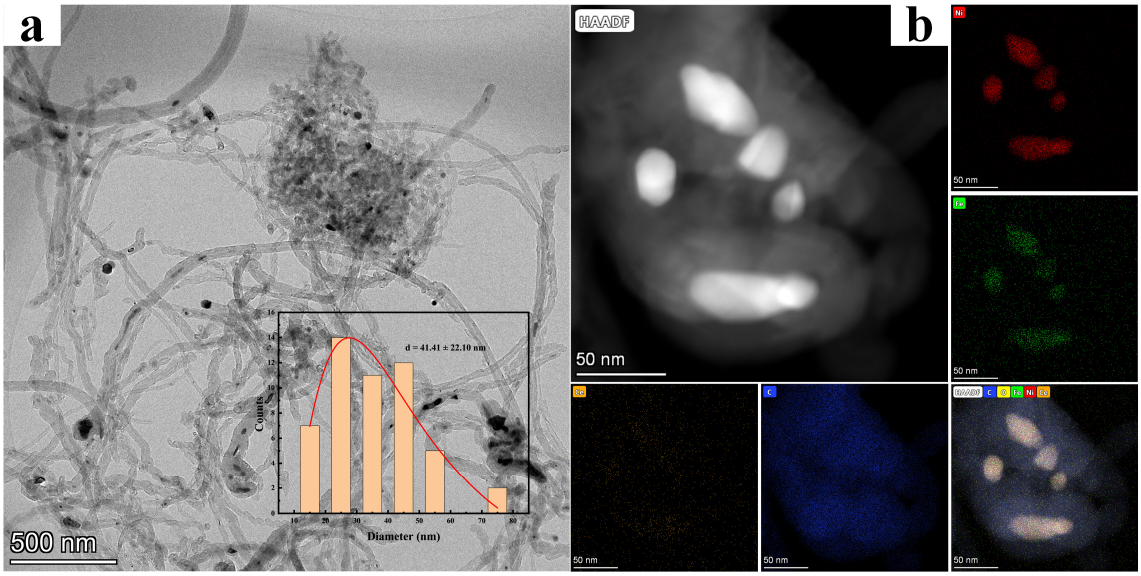

Fig. S11 TEM (a) HAADF-STEM images and mapping (b) images of the spent Ni_3Fe/CeO_2-NS catalyst.

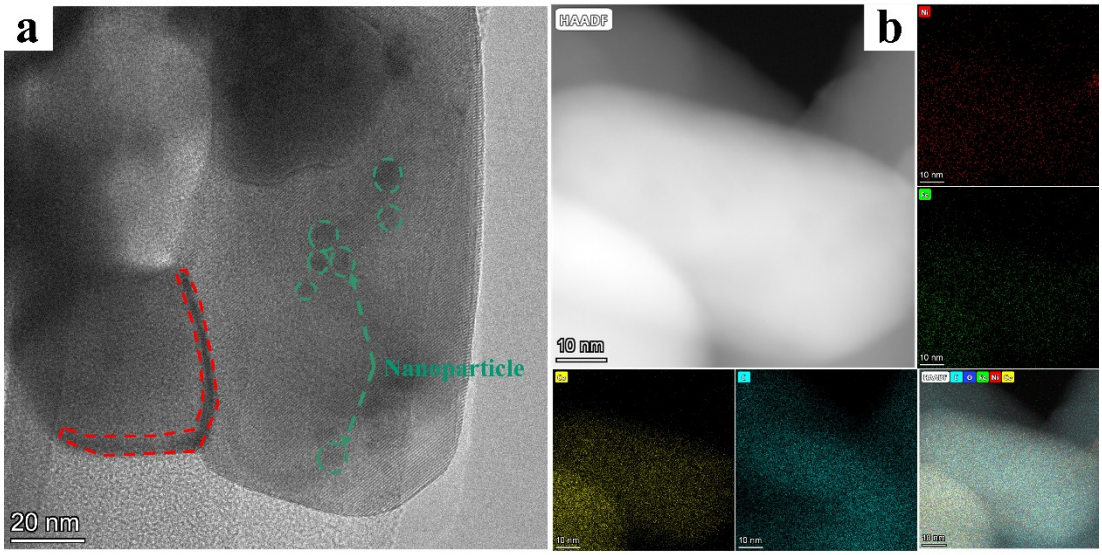

Fig. S12 TEM (a) HAADF-STEM images and mapping (b) images of the spent Ni_3Fe/CeO_2-RS catalyst.

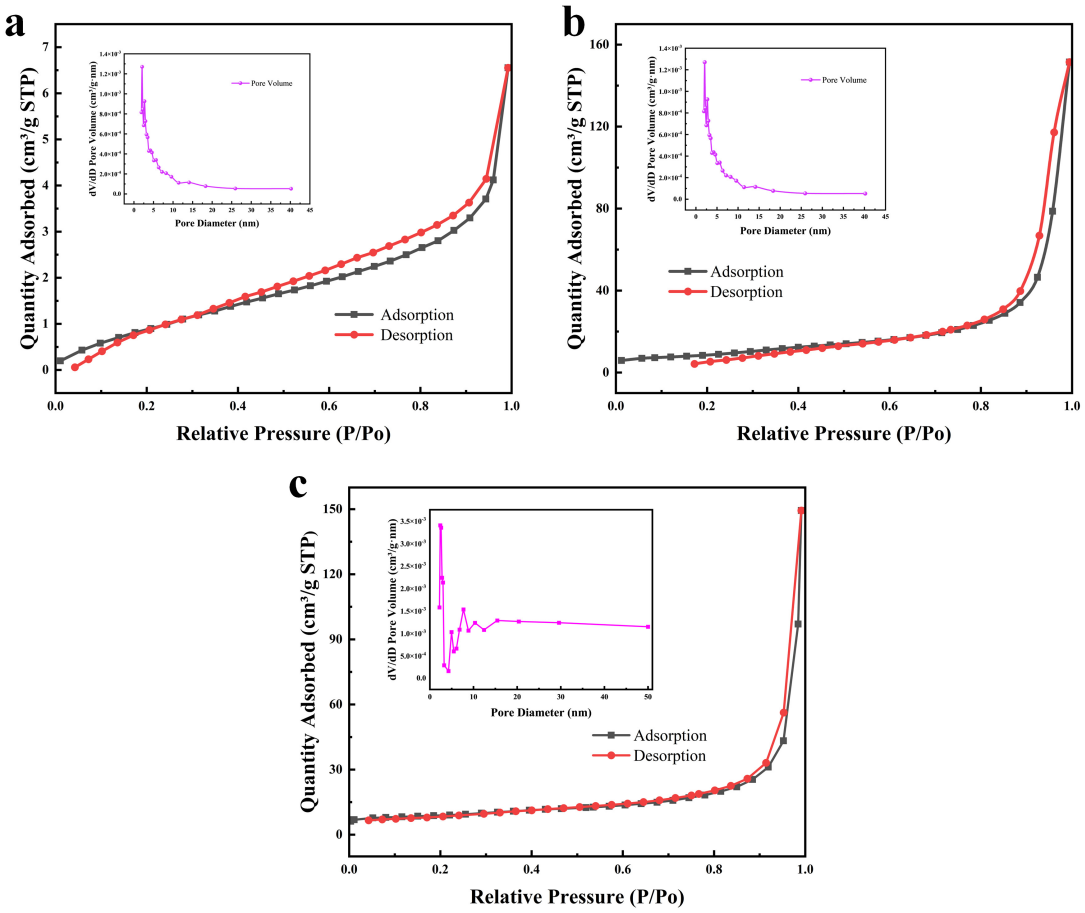

Fig. S13 N_2 sorption isotherms and pore diameter distribution of Ni_3Fe/CeO_2 (a), Ni_3Fe/CeO_2-NS (b) and Ni_3Fe/CeO_2-RS (c) after reaction, respectively

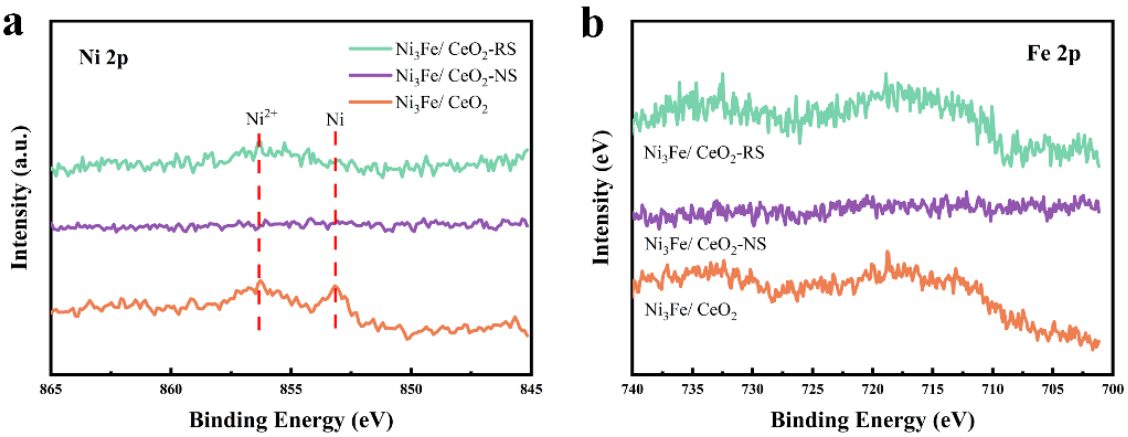

Fig. S14 Ni 2p and Fe 2p XPS spectrums of the spent catalysts.

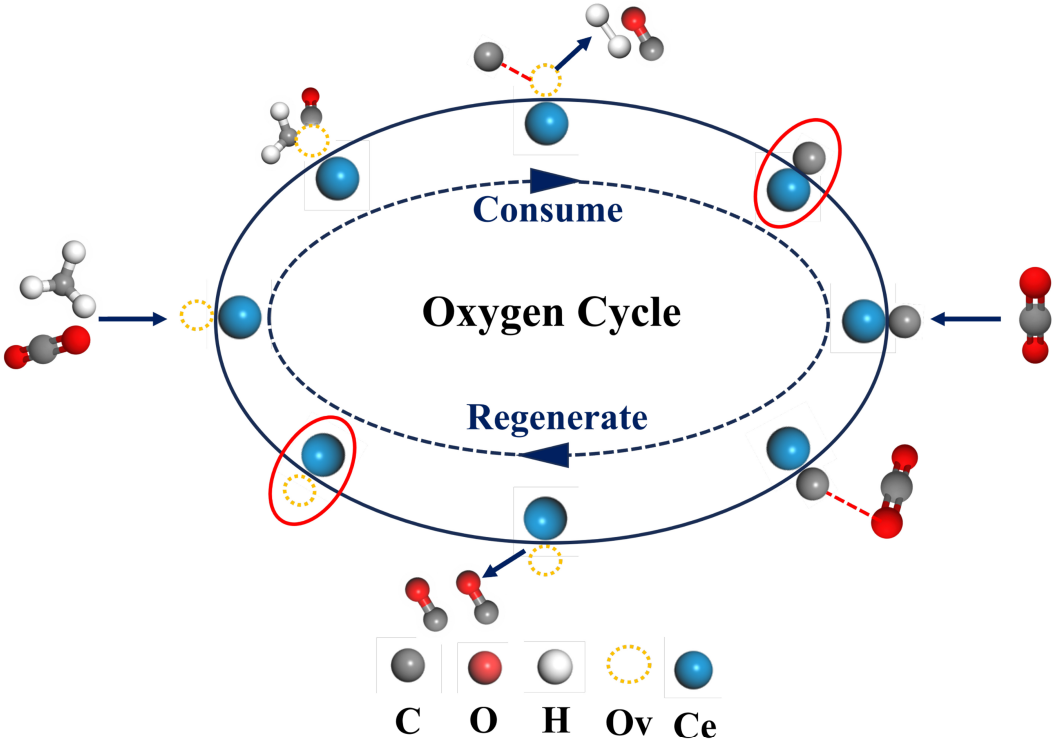

Fig. S15 schematic diagram of the catalytic mechanism.

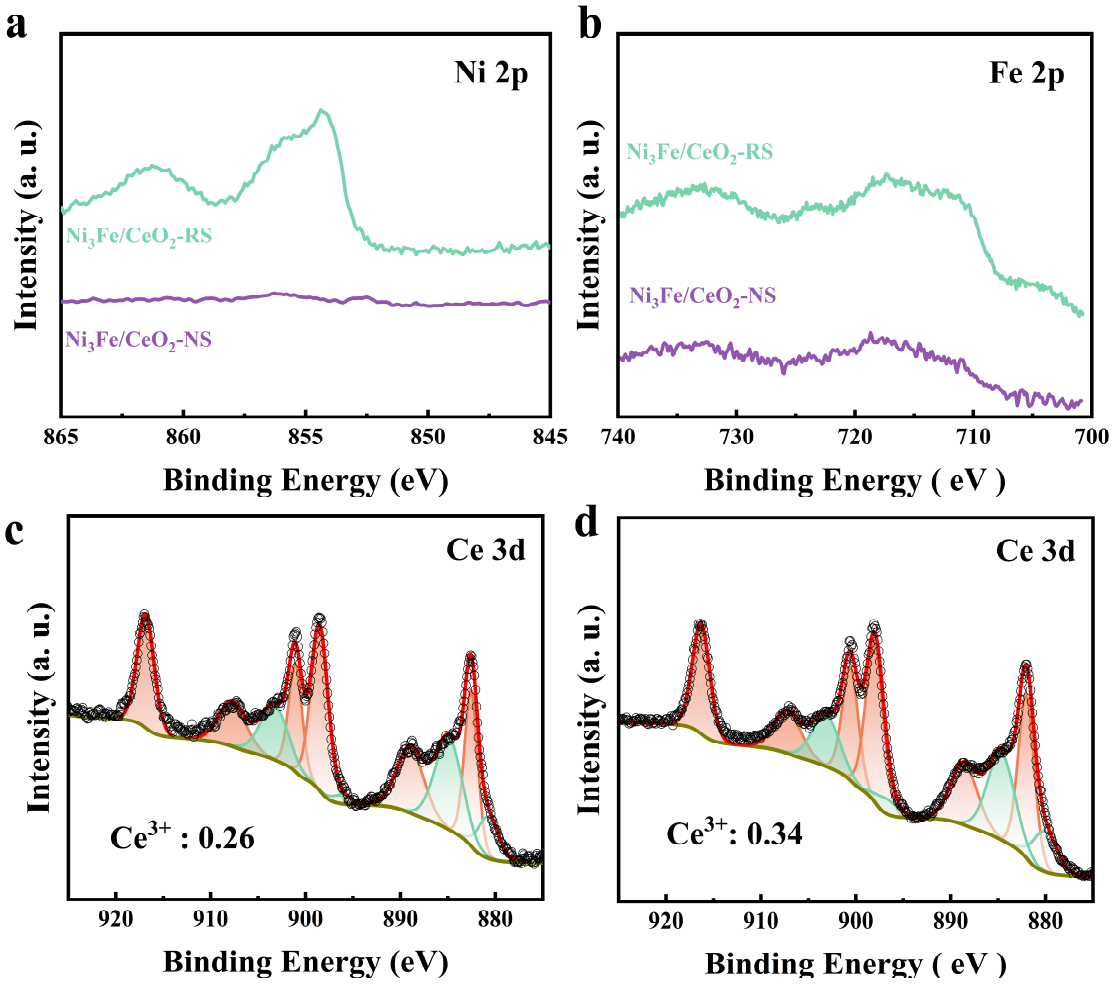

Fig. S16 XPS spectrum after the first cycle reaction. (a) Ni 2p, (b) Fe 2p, (c) Ce 3d of Ni_3Fe/CeO_2-NS, (d) Ce 3d of Ni_3Fe/CeO_2-RS